CLASSIFICATION AND CLUSTERING OF SEQUENCING DATA USING A POISSON MODEL

By Daniela M. Witten

University of Washington

In recent years, advances in high throughput sequencing technology have led to a need for specialized methods for the analysis of digital gene expression data. While gene expression data measured on a microarray take on continuous values and can be modeled using the normal distribution, RNA sequencing data involve nonnegative counts and are more appropriately modeled using a discrete count distribution, such as the Poisson or the negative binomial. Consequently, analytic tools that assume a Gaussian distribution (such as classification methods based on linear discriminant analysis and clustering methods that use Euclidean distance) may not perform as well for sequencing data as methods that are based upon a more appropriate distribution. Here, we propose new approaches for performing classification and clustering of observations on the basis of sequencing data. Using a Poisson log linear model, we develop an analog of diagonal linear discriminant analysis that is appropriate for sequencing data. We also propose an approach for clustering sequencing data using a new dissimilarity measure that is based upon the Poisson model. We demonstrate the performances of these approaches in a simulation study, on three publicly available RNA sequencing data sets, and on a publicly available chromatin immunoprecipitation sequencing data set.

1. Introduction.

1.1. *An overview of RNA sequencing data.* Since the late 1990s, a vast literature has been devoted to quantifying the extent to which different tissue types, biological conditions, and disease states are characterized by particular patterns of gene expression, or mRNA levels [examples include DeRisi, Iyer and Brown (1997), Spellman et al. (1998), Brown and Botstein (1999), Ramaswamy et al. (2001), Nielsen et al. (2002), Monti et al. (2005)].

1

During most of that time, the microarray has been the method of choice for quantifying gene expression. Though the microarray has led to an improved understanding of many cellular processes and disease states, the technology suffers from two fundamental limitations:

(1) Cross-hybridization can occur, whereby cDNA hybridizes to a probe for which it is not perfectly matched. This can lead to high levels of background noise.

(2) Only transcripts for which a probe is present on the array can be measured. Therefore, it is not possible to discover novel mRNAs in a typical microarray experiment.

In recent years, *high throughput* or *second generation* RNA sequencing has emerged as a powerful alternative to the microarray for measuring gene expression [see, e.g., Mortazavi et al. (2008), Nagalakshmi et al. (2008), Wilhelm and Landry (2009), Wang, Gerstein and Snyder (2009), Pepke, Wold and Mortazavi (2009)]. This technology allows for the parallel sequencing of a large number of mRNA transcripts. Briefly, RNA sequencing proceeds as follows [Mortazavi et al. (2008), Morozova, Hirst and Marra (2009), Wang, Gerstein and Snyder (2009), Auer and Doerge (2010), Oshlack, Robinson and Young (2010)]:

(1) RNA is isolated and fragmented to an average length of 200 nucleotides.

(2) The RNA fragments are converted into cDNA.

(3) The cDNA is sequenced.

This process results in millions of short reads, between 25 and 300 basepairs in length, usually taken from one end of the cDNA fragments (though some technologies result in "paired-end" reads). The reads are typically then mapped to the genome or transcriptome if a suitable reference genome or transcriptome is available; if not, then *de novo* assembly may be required [Oshlack, Robinson and Young (2010)]. The mapped reads can then be pooled into regions of interest. For instance, reads may be pooled by gene or by exon, in which case the data consist of nonnegative counts indicating the number of reads observed for each gene or each exon. In this paper we will assume that mapping and pooling of the raw reads has already been performed. We will consider RNA data sets that take the form of $n \times p$ matrices, where n indicates the number of samples for which sequencing was performed, and p indicates the number of regions of interest (referred to as "features"). The (i, j) element of the data matrix indicates the number of reads from the ith sample that mapped to the jth region of interest. Sequencing data are generally very high dimensional, in the sense that the number of features p is much larger than the number of observations n. Specifically, p is usually on the order of tens of thousands, if not much larger.

RNA sequencing has some major advantages over the microarray. RNA sequencing data should in theory be much less noisy than microarray data, since the technology does not suffer from cross-hybridization. Moreover, novel transcripts and coding regions can be discovered using RNA sequencing, since unlike studies performed using microarrays, sequencing experiments do not require pre-specification of the transcripts of interest. For these reasons, it seems certain that RNA sequencing is on track to replace the microarray as the technology of choice for the characterization of gene expression.

1.2. *Statistical models for RNA sequencing data.* Two aspects of sequencing data are especially worth noting, as they result in unique statistical challenges. (1) Due to artifacts of the sequencing experiment, different samples can have vastly different total numbers of sequence reads. This issue is generally addressed by normalizing the samples in some way, for instance, by the total number of reads observed for each sample [Mortazavi et al. (2008)] or a more robust alternative [Bullard et al. (2010), Robinson and Oshlack (2010), Anders and Huber (2010)]. Simply dividing the counts for a given sample by a normalization constant may not be desirable, since the magnitude of the counts may contain information about the variability in the data. (2) Since a sequencing data set consists of the number of reads mapping to a particular region of interest in a particular sample, the data are integer-valued and nonnegative. This is in contrast to microarray data, which is measured on a continuous scale and can reasonably be modeled using a Gaussian distribution.

Let $\mathbf{X}$ denote a $n \times p$ matrix of sequencing data, with n observations (e.g., tissue samples) and p features (regions of interest; e.g., genes or exons). X_{ij} is the count for feature j in observation i. For instance, if feature j is a gene, then X_{ij} is the total number of reads mapping to gene j in observation i. A number of authors have considered a Poisson log linear model for sequencing data,

$$(1) \qquad X_{ij} \sim \text{Poisson}(N_{ij}), \qquad N_{ij} = s_i g_j$$

[among others, Marioni et al. (2008), Bullard et al. (2010), Witten et al. (2010), Li et al. (2011)]. To avoid identifiability issues, one can require $\sum_{i=1}^{n} s_i = 1$. This model allows for variability in both the total number of reads per sample (via the s_i term) and in the total number of reads per region of interest (via the g_j term). Since biological replicates seem to be overdispersed relative to the Poisson model, some authors have proposed an extension to (1) involving the use of a negative binomial model, a natural alternative to the Poisson model that allows for the variance to exceed the mean [among others, Robinson, McCarthy and Smyth (2010), Anders and

Huber ([2010](#))]. Specifically, one could extend ([1](#)) to obtain

$$(2) \qquad X_{ij} \sim \text{NB}(N_{ij}, \phi_j), \qquad N_{ij} = s_i g_j,$$

where NB indicates the negative binomial distribution and $\phi_j \geq 0$ is the dispersion parameter for feature j. Throughout this paper, the negative binomial distribution will be parametrized such that ([2](#)) implies that observation X_{ij} has mean N_{ij} and variance $N_{ij} + N_{ij}^2 \phi_j$. When $\phi_j = 0$, ([2](#)) reduces to ([1](#)).

RNA sequencing experiments are often designed such that the n observations are drawn from K different biological conditions, or *classes*. To accommodate this setting, a number of authors have extended ([1](#)) and ([2](#)) as follows:

$$(3) \qquad X_{ij}|y_i = k \sim \text{Poisson}(N_{ij}d_{kj}), \qquad N_{ij} = s_i g_j,$$

$$(4) \qquad X_{ij}|y_i = k \sim \text{NB}(N_{ij}d_{kj}, \phi_j), \qquad N_{ij} = s_i g_j,$$

where y_i indicates the class of the ith observation, $y_i \in \{1, \ldots, K\}$. Here the $d_{1j}, \ldots, d_{Kj}$ terms allow the jth feature to be differentially expressed between classes. [However, as written in ([3](#)) and ([4](#)), the precise roles of $d_{1j}, \ldots, d_{Kj}$ are difficult to interpret because the model is overparametrized. We will address this point in Section [2.1](#).] The models ([3](#)) and ([4](#)) have been used to identify features that are differentially expressed between conditions [Marioni et al. ([2008](#)), Bullard et al. ([2010](#)), Witten et al. ([2010](#)), Li et al. ([2011](#)), Robinson, McCarthy and Smyth ([2010](#)), Anders and Huber ([2010](#))].

Though the question of how best to identify differentially expressed features has now been extensively studied, it is just one of many possible scientific questions that may arise from sequencing data. This paper addresses the following two problems:

(1) If each sample is associated with a class label, then one might wish to build a classifier in order to predict the class label of a future observation.

(2) If the samples are unlabeled, one might wish to cluster the samples in order to identify subgroups among them.

Most of the methods in the statistical literature for classification and clustering implicitly assume a normal distribution for the data. In this paper, due to the nature of sequencing data, the Poisson log linear models ([1](#)) and ([3](#)) will be used to accomplish these two tasks. The importance of the model used can be seen on a simple toy example. We generated two-dimensional Poisson distributed random variables with two different means, each representing a different class. Each dimension was generated independently. The Bayes-optimal decision boundaries obtained assuming normality and assuming a Poisson distribution are shown in Figure [1](#).
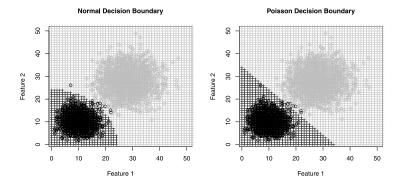
FIG. 1. *Two sets of two-dimensional independent random variables were generated. The first set of random variables was generated according to the* Poisson(10) *distribution in each dimension, and the second set was generated according to the* Poisson(28) *distribution in each dimension. In each figure, the two sets of random variables are shown as black and grey circles, after jittering. The grid in the background of each plot indicates the Bayes-optimal decision boundary, assuming a normal distribution (left) or a Poisson distribution (right) with the correct mean and variance.*

1.3. *Notation and organization.* The following additional notation will be used in this paper. Let $\mathbf{x}_i = (X_{i1} \cdots X_{ip})^T$ denote row i of $\mathbf{X}$, corresponding to the feature measurements for observation i. Also, $X_{\cdot j} = \sum_{i=1}^{n} X_{ij}$, $X_{i\cdot} = \sum_{j=1}^{p} X_{ij}$, $X_{\cdot\cdot} = \sum_{i,j} X_{ij}$. Moreover, in the classification setting where each observation belongs to one of K classes, we let $C_k \subset \{1, \ldots, n\}$ contain the indices of the observations in class k—that is, $y_i = k$ if and only if $i \in C_k$. Furthermore, $X_{C_k j} = \sum_{i \in C_k} X_{ij}$.

The rest of this paper is organized as follows. In Section 2 the model (3) is presented in greater detail, along with methods for fitting it that are based upon recent proposals in the literature. This model is used as the basis for the classifier proposed in Section 3 and as the basis for the clustering method proposed in Section 4. In Section 5 the performances of the classification and clustering proposals are evaluated in a simulation study. The proposals are applied to four sequencing data sets in Section 6. Section 7 contains the Discussion.

2. A Poisson log linear model for multiple-class sequencing data.

2.1. *The model.* In this paper sequencing data are modeled using a Poisson log linear model. However, the proposals in this paper could be extended to the negative binomial model using techniques developed in Robinson, McCarthy and Smyth (2010) and Anders and Huber (2010).

The model (1) captures the fact that sequencing data are characterized by high levels of variation in both the number of counts per sample (s_i) and the number of counts per feature (g_j), and (3) additionally allows for the

level of expression of a given feature to depend upon the condition under which it is observed $(d_{1j}, \ldots, d_{Kj})$. Throughout this paper, we assume that the X_{ij}'s are independent of each other for all $i = 1, \ldots, n$, $j = 1, \ldots, p$.

We first consider the problem of fitting the model (1). The maximum likelihood estimate (MLE) for N_{ij} is $\hat{N}_{ij} = \frac{X_{i\cdot}X_{\cdot j}}{X_{\cdot\cdot}}$ [Agresti (2002)]. Combining this with the identifiability constraint that $\sum_{i=1}^{n} \hat{s}_i = 1$ yields the estimates $\hat{s}_i = X_{i\cdot}/X_{\cdot\cdot}$ and $\hat{g}_j = X_{\cdot j}$. We can interpret $\hat{s}_i$ as an estimate of the *size factor* for sample i, reflecting the fact that different samples may have been sequenced to different depths. A number of authors have used this size factor estimate [Marioni et al. (2008), Mortazavi et al. (2008)]. Recently, it has been pointed out that $X_{i\cdot}/X_{\cdot\cdot}$ is not a very good estimate for s_i since changes in a few high-count features can have a great effect on the value of $X_{i\cdot}$, skewing any resulting analyses [Bullard et al. (2010), Robinson and Oshlack (2010), Anders and Huber (2010), Li et al. (2011)]. For this reason, several more robust estimates for the size factor s_i have been proposed. In what follows we will consider three estimates for s_i:

(1) *Total count.* We simply use $\hat{s}_i = X_{i\cdot}/X_{\cdot\cdot}$, the total count for the ith observation, which is based upon the MLE for N_{ij} under the model (1).

(2) *Median ratio.* Anders and Huber (2010) propose the use of $\hat{s}_i = m_i / \sum_{i=1}^{n} m_i$, where

$$\text{(5)} \qquad m_i = \text{median}_j \left\{ \frac{X_{ij}}{(\prod_{i'=1}^{n} X_{i'j})^{1/n}} \right\}.$$

That is, the size factor for the ith sample is obtained by computing the median, over all p features, of the ith sample count for that feature divided by the geometric mean of all sample counts for that feature.

(3) *Quantile.* Bullard et al. (2010) propose taking $\hat{s}_i = q_i / \sum_{i=1}^{n} q_i$, where q_i is the 75th percentile of the counts for each sample.

Thus, throughout this paper, we will estimate N_{ij} in (1) according to $\hat{N}_{ij} = \hat{s}_i \hat{g}_j$, where $\hat{s}_i$ is given by one of the methods described above, and $\hat{g}_j = X_{\cdot j}$.

We now consider the problem of fitting the model (3). Since we would like to attribute as much as possible of the observed variability in the counts for each feature to sample and feature effects (s_i and g_j) rather than to class differences (d_{kj}), we estimate N_{ij} under the model (1) without making use of the class labels. We then estimate d_{kj} by treating $\hat{N}_{ij}$ as an offset in the model (3). That is, we fit the model

$$\text{(6)} \qquad X_{ij} | y_i = k \sim \text{Poisson}(\hat{N}_{ij} d_{kj}).$$

Maximum likelihood provides a natural way to estimate d_{kj} in (6), yielding $\hat{d}_{kj} = \frac{X_{C_k j}}{\sum_{i \in C_k} \hat{N}_{ij}}$. Now $\hat{d}_{kj}$ has a simple interpretation: if $\hat{d}_{kj} > 1$, then the jth feature is over-expressed relative to the baseline in the kth class, and if

$\hat{d}_{kj} < 1$, then the jth feature is under-expressed relative to the baseline in the kth class.

However, if $X_{C_k j} = 0$ (an event that is not unlikely if the true mean for feature j is small), then the maximum likelihood estimate for d_{kj} equals zero. This can pose a problem for downstream analyses, since this estimate completely precludes the possibility of a nonzero count for feature j arising from an observation in class k. We can remedy this problem by putting a Gamma(β, β) prior on d_{kj} in the model (6). Here, the shape and rate parameters both equal β. Then, the posterior distribution for d_{kj} is Gamma$(X_{C_k j} + \beta, \sum_{i \in C_k} \hat{N}_{ij} + \beta)$, and the posterior mean is

$$(7) \qquad \hat{d}_{kj} = \frac{X_{C_k j} + \beta}{\sum_{i \in C_k} \hat{N}_{ij} + \beta}.$$

Equation (7) is a smoothed estimate of d_{kj} that behaves well even if $X_{C_k j} = 0$ for some class k. We took $\beta = 1$ in all of the examples shown in this paper.

2.2. *A transformation for overdispersed data.* A number of authors have observed that, in practice, biological replicates of sequencing data tend to be overdispersed relative to the Poisson model, in the sense that the variance is larger than the mean. This problem could be addressed by using a different model for the data, such as a negative binomial model [Robinson, McCarthy and Smyth (2010), Anders and Huber (2010)]. Instead, we apply a power transformation to the data [Witten et al. (2010), Li et al. (2011)]. The transformation $X'_{ij} \leftarrow X^\alpha_{ij}$ is used, where $\alpha \in (0, 1]$ is chosen so that

$$(8) \qquad \sum_{i=1}^n \sum_{j=1}^p \frac{(X'_{ij} - X'_{i.}X'_{.j}/X'_{..})^2}{X'_{i.}X'_{.j}/X'_{..}} \approx (n-1)(p-1).$$

This is simply a test of the goodness of fit of the model (1) to the data [Agresti (2002)], using the total count size factor estimate $\hat{s}_i = X'_{i.}/X'_{..}$.

Though the resulting transformed data are not integer-valued, we nonetheless model them using the Poisson distribution. This simple transformation allows us to use a Poisson model even in the case of overdispersed data, in order to avoid having to fit a necessarily more complicated negative binomial model (a task made especially complicated in the typical setting for sequencing data where the number of samples is small). In Section 5 we show that even when data are generated according to a negative binomial model with moderate overdispersion, the classification and clustering proposals based on the Poisson model perform well on the transformed data.

3. A proposal for classifying sequencing data.

3.1. *The Poisson linear discriminant analysis classifier.* Suppose that we wish to classify a test observation $\mathbf{x}^* = (X_1^* \cdots X_p^*)^T$ on the basis of

training data $\{(\mathbf{x}_i, y_i)\}_{i=1}^n$. Let y^* denote the unknown class label. By Bayes' rule,

$$(9) \qquad P(y^* = k|\mathbf{x}^*) \propto f_k(\mathbf{x}^*)\pi_k,$$

where f_k is the density of an observation in class k and π_k is the prior probability that an observation belongs to class k. If f_k is a normal density with a class-specific mean and common covariance, then assigning an observation to the class for which (9) is largest results in standard LDA [for a reference, see Hastie, Tibshirani and Friedman (2009)]. If we instead assume that the observations are normally distributed with a class-specific mean and a common diagonal covariance matrix, then diagonal LDA results [Dudoit, Fridlyand and Speed (2001)]. The assumption of normality is not appropriate for sequencing data, and neither is the assumption of a common covariance matrix for the K classes. We instead assume that the data arise from the model (3), and we also assume that the features are independent. The assumption of independence is often made for high-dimensional continuous data [e.g., see Dudoit, Fridlyand and Speed (2001), Tibshirani et al. (2002, 2003), Bickel and Levina (2004), Witten and Tibshirani (2011)] since when $p > n$, there are too few observations available to be able to effectively estimate the dependence structure among the features.

Evaluating (9) requires estimation of $f_k(\mathbf{x}^*)$ and π_k. The model (3) states that $X_j^*|y^* = k \sim \text{Poisson}(s^* g_j d_{kj})$. We first estimate $s_1, \ldots, s_n$, the size factors for the training data, using the total count, quantile, or median ratio approaches (Section 2.1). We then estimate g_j and d_{kj} by evaluating $\hat{g}_j = X_{\cdot j}$ and (7) on the training data. Finally, we estimate s^* as follows:

- If the total count estimate for the size factors was used, then $\hat{s}^* = \sum_{j=1}^p X_j^* / X_{\cdot\cdot}$, where $X_{\cdot\cdot}$ is the total number of counts on the *training* data.
- If the median ratio estimate for the size factors was used, then $\hat{s}^* = m^* / \sum_{i=1}^n m_i$, where $m^* = \text{median}_j \{ \frac{X_j^*}{(\prod_{i=1}^n X_{ij})^{1/n}} \}$—note that the denominator is the geometric mean for the jth feature among the *training* observations. Here m_i is given by (5).
- If the quantile estimate for the size factors was used, then $\hat{s}^* = q^* / \sum_{i=1}^n q_i$. Here, q^* is the 75th percentile of counts for the test observation, and q_i is the 75th percentile of counts for the ith training observation.

Note that these estimates of s^* are the direct extensions of the size factor estimates presented in Section 2.1, applied to the test observation $\mathbf{x}^*$.

We now consider the problem of estimating π_k. We could let $\hat{\pi}_1 = \cdots = \hat{\pi}_K = 1/K$, corresponding to the prior that all classes are equally likely. Alternatively, we could let $\hat{\pi}_k = |C_k|/n$, if we believe that the proportion of observations in each class seen in the training set is representative of the proportion in the population. In the examples presented in Sections 5 and 6, we take $\hat{\pi}_1 = \cdots = \hat{\pi}_K = 1/K$.

Plugging these estimates into (3) and recalling our assumption of independent features, (9) yields

(10)
$$\log P(\widehat{y^* = k}|\mathbf{x}^*) = \log \hat{f}_k(\mathbf{x}^*) + \log \hat{\pi}_k + c$$
$$= \sum_{j=1}^p X_j^* \log \hat{d}_{kj} - \hat{s}^* \sum_{j=1}^p \hat{g}_j \hat{d}_{kj} + \log \hat{\pi}_k + c',$$

where c and c' are constants that do not depend on the class label. Only the first term in (10) involves the individual feature measurements for the test observation $\mathbf{x}^*$. Therefore, the classification rule that assigns the test observation to the class for which (10) is largest is linear in $\mathbf{x}^*$. For this reason, we call this classifier *Poisson linear discriminant analysis* (PLDA). This name reflects the linearity of the classifier, as well as the fact that it differs from standard LDA only in its use of a Poisson model for the data.

3.2. *The sparse PLDA classifier.* PLDA's classification rule (10) is quite simple, in that it is linear in the components of $\mathbf{x}^*$. But when the estimate (7) is used for d_{kj}, then $\hat{d}_{kj} \neq 1$ in general and so the classification rule (10) involves all p features. For sequencing data, p may be quite large, and a classifier that involves only a subset of the features is desirable in order to achieve increased interpretability and reduced variance. By inspection, the classification rule (10) will not involve the data for feature j if $\hat{d}_{1j} = \cdots = \hat{d}_{Kj} = 1$. We obtain a classification rule that is sparse in the features by using the following estimate for d_{kj} in (10), which shrinks the estimate (7) toward 1:

(11)
$$\hat{d}_{kj} = \begin{cases} \frac{a}{b} - \frac{\rho}{\sqrt{b}}, & \text{if } \sqrt{b}\left(\frac{a}{b} - 1\right) > \rho, \\ \frac{a}{b} + \frac{\rho}{\sqrt{b}}, & \text{if } \sqrt{b}\left(1 - \frac{a}{b}\right) > \rho, \\ 1, & \text{if } \sqrt{b}\left|1 - \frac{a}{b}\right| < \rho, \end{cases}$$

where $a = X_{C_k j} + \beta$ and $b = \sum_{i \in C_k} \hat{N}_{ij} + \beta$. Here, ρ is a nonnegative tuning parameter that is generally chosen by cross-validation. When $\rho = 0$, (11) is simply the estimate (7). As ρ increases, so does the number of estimates (11) that are exactly equal to 1. Using the estimate (11) in the PLDA classifier (10) yields *sparse PLDA (sPLDA)*. The operation (11) can be written more concisely as $\hat{d}_{kj} = 1 + S(a/b - 1, \rho/\sqrt{b})$, where S is the soft-thresholding operator, given by $S(x, a) = \text{sign}(x)(|x| - a)_+$. Note that the form of (11) combined with the definition of b implies that if class k contains few observations, or if the mean for class k in feature j is small, then the estimate for d_{kj} will undergo greater shrinkage.

Sparse PLDA is closely related to the nearest shrunken centroids (NSC) classifier [Tibshirani et al. (2002, 2003)], which is a variant of diagonal LDA that arises from shrinking the class-specific mean vectors toward a common mean using the soft-thresholding operator. In fact, sPLDA arises from replacing the normal model that leads to NSC with the Poisson model (3). For this reason, NSC is a natural method against which to compare sPLDA.

4. A proposal for clustering sequencing data.

4.1. *Poisson dissimilarity.* We now consider the problem of computing a $n \times n$ dissimilarity matrix for n observations for which sequencing measurements are available. For microarray data, squared Euclidean distance is a common choice of dissimilarity measure. Another popular choice, correlation-based distance, is equivalent to squared Euclidean distance up to a scaling of the observations [Hastie, Tibshirani and Friedman (2009)]. Squared Euclidean distance can be derived as the consequence of performing hypothesis testing on a simple Gaussian model for the data. That is, consider the model

$$
(12) \qquad X_{ij} \sim N(\mu_{ij}, \sigma^2), \qquad X_{i'j} \sim N(\mu_{i'j}, \sigma^2),
$$

where we assume that the features and observations are independent. Consider testing the null hypothesis $H_0 : \mu_{ij} = \mu_{i'j}, j = 1, \ldots, p$, against H_a, which states that μ_{ij} and $\mu_{i'j}$ are unrestricted. The resulting log likelihood ratio statistic is proportional to

$$
\sum_{j=1}^{p} \left(X_{ij} - \frac{X_{ij} + X_{i'j}}{2} \right)^2 + \sum_{j=1}^{p} \left(X_{i'j} - \frac{X_{ij} + X_{i'j}}{2} \right)^2 \propto \sum_{j=1}^{p} (X_{ij} - X_{i'j})^2
$$
$$
(13) \qquad\qquad\qquad\qquad\qquad\qquad\qquad\qquad\qquad\qquad\qquad\qquad = \|\mathbf{x}_i - \mathbf{x}_{i'}\|^2.
$$

Therefore, squared Euclidean distance is equivalent to a log likelihood ratio statistic for each pair of observations, under a Gaussian model for the data.

Now, as discussed earlier, the model (12) does not seem appropriate for sequencing data. Instead, consider the model

$$
(14) \qquad
\begin{aligned}
X_{ij} &\sim \text{Poisson}(N_{ij} d_{ij}), \qquad X_{i'j} \sim \text{Poisson}(N_{i'j} d_{i'j}), \\
N_{ij} &= s_i g_j, \qquad N_{i'j} = s_{i'} g_j,
\end{aligned}
$$

where we assume that the features are independent. This is simply the model (3), restricted to $\mathbf{x}_i$ and $\mathbf{x}_{i'}$. We first estimate $N_{ij}, N_{i'j}$ under the simpler model

$$
(15) \qquad
\begin{aligned}
X_{ij} &\sim \text{Poisson}(N_{ij}), \qquad X_{i'j} \sim \text{Poisson}(N_{i'j}), \\
N_{ij} &= s_i g_j, \qquad N_{i'j} = s_{i'} g_j
\end{aligned}
$$

as described in Section 2.1—using total count, quantile, or median ratio size factor estimates—but restricted to $\mathbf{x}_i$ and $\mathbf{x}_{i'}$. We then test the null hypothesis $H_0 : d_{ij} = d_{i'j} = 1, j = 1, \ldots, p$, against the alternative H_a, which states that d_{ij} and $d_{i'j}$ are nonnegative. The resulting log likelihood ratio statistic can be used as a measure of dissimilarity between $\mathbf{x}_i$ and $\mathbf{x}_{i'}$. A standard log likelihood ratio statistic would involve computing the maximum likelihood estimates for d_{ij} and $d_{i'j}$ under H_a. However, to avoid the estimate $\hat{d}_{ij} = 0$ if $X_{ij} = 0$, we instead compute a *modified* log likelihood ratio statistic: we evaluate the log likelihood under H_a using the estimates

$$(16) \qquad \hat{d}_{ij} = \frac{X_{ij} + \beta}{\hat{N}_{ij} + \beta}, \qquad \hat{d}_{i'j} = \frac{X_{i'j} + \beta}{\hat{N}_{i'j} + \beta},$$

which are the posterior means for d_{ij} and $d_{i'j}$ under Gamma(β, β) priors. The resulting modified log likelihood ratio statistic is

$$(17) \qquad \sum_{j=1}^{p} (\hat{N}_{ij} + \hat{N}_{i'j} - \hat{N}_{ij}\hat{d}_{ij} - \hat{N}_{i'j}\hat{d}_{i'j} + X_{ij} \log \hat{d}_{ij} + X_{i'j} \log \hat{d}_{i'j}).$$

Then (17) can be thought of as the dissimilarity between $\mathbf{x}_i$ and $\mathbf{x}_{i'}$ under the model (3). The dissimilarity between two identical observations is 0, and all dissimilarities are nonnegative (see the Appendix). We will refer to the $n \times n$ dissimilarity matrix with (i, j) element given by (17) as the *Poisson dissimilarity* matrix.

Hierarchical clustering is a very popular approach for clustering in genomics since it leads to a visual representation of the data and does not require prespecifying the number of clusters. Hierarchical clustering operates on a $n \times n$ dissimilarity matrix, and can be performed using the Poisson dissimilarity matrix. We will refer to the clustering obtained using this dissimilarity matrix as *Poisson clustering*.

To obtain a $p \times p$ Poisson dissimilarity matrix of the features rather than a $n \times n$ dissimilarity matrix of the observations, one could use a Poisson model and repeat the arguments in this section, reversing the roles of observations and features in each of the relevant equations. One could then use this dissimilarity matrix in order to perform Poisson clustering of the features.

4.2. *Alternative approaches for clustering count data.* We briefly review some approaches from the literature for computing dissimilarity matrices or performing clustering using count data.

Serial analysis of gene expression (SAGE) is a sequencing-based method for gene expression profiling that predates RNA sequencing [Wang (2007)]. In SAGE a prespecified region of the RNA transcript is sequenced, and so the ability to detect previously unknown RNA transcripts is somewhat

limited. Cai et al. ([2004](#)) propose a procedure for performing K-means clustering of SAGE data using a Poisson model. Though their approach focuses on clustering features (known as *tags* in the context of SAGE data) rather than observations, their approach is fundamentally very similar to the one proposed here in that a Poisson model is used and deviations from the Poisson model (measured using a chi-squared statistic or the log likelihood) are taken as an indication that two tags are different from each other and hence belong in different clusters. They propose to fit the Poisson model using the maximum likelihood parameter estimates, which is analogous to using total count size factor estimates in our model. They fit the Poisson model using all n observations at once rather than separately for each pair of observations as in ([15](#)). In our experience, fitting the model separately for each pair of observations leads to better results. Their approach yields a prespecified number of clusters K, whereas ours yields a dissimilarity matrix that can be hierarchically clustered to obtain any number of clusters, or used for other purposes.

Berninger et al. ([2008](#)) propose a method for computing a dissimilarity matrix using sequencing data that is also very closely related to ours. They assume that each observation is drawn from a multinomial distribution, and they test whether or not the multinomial parameters for each pair of observations are equal. This is almost identical to our Poisson model and associated hypothesis testing framework, since if the observations are distributed according to ([14](#)), then their distribution conditional on $X_{i\cdot}$, $X_{i'\cdot}$ is multinomial. In fact, the log likelihood ratio statistics under our model and theirs are identical for certain very natural estimates of N_{ij}, $N_{i'j}$, d_{ij}, and $d_{i'j}$ in ([17](#)) (see the [Appendix](#)). However, there are some important differences between the two proposals. Berninger et al. ([2008](#)) place a Dirichlet prior on the parameters for the multinomial distribution, and then use a Bayes factor as a measure of the dissimilarity between two observations. Consequently, two identical observations can have nonzero dissimilarity according to Berninger et al. ([2008](#)), and two different observations can have smaller dissimilarity than two identical observations. This leads to problems in the interpretation of their dissimilarity measure as well as in the performance of any clustering approach that is based upon it. Finally, their approach can suffer from numerical issues where the computed dissimilarity between a pair of observations rounds to zero.

The edgeR software package, available from Bioconductor [Robinson, McCarthy and Smyth ([2010](#))], provides a tool for measuring the dissimilarity between a pair of observations based upon a negative binomial model. The q features with highest feature-wise dispersion across all n samples are selected, and the common dispersion of those q features for each pair of observations is used as a measure of pairwise dissimilarity.

TABLE 1

Summary of approaches for computing dissimilarity measures

Method	Description
EdgeR	A proposal in the edgeR software package, based on a negative binomial model [Robinson, McCarthy and Smyth (2010)]. The dissimilarity between a pair of observations is computed as the common dispersion of the 500 features with the highest feature-wise dispersion across all n samples.
Berninger	An approach for computing dissimilarities between pairs of observations, using a multinomial model with a Dirichlet prior [Berninger et al. (2008)].
VST	A variance stabilizing transformation (VST) based on a negative binomial model [Anders and Huber (2010)] is applied to the data, and then squared Euclidean distances between pairs of observations are computed.
Sq. Euclidean total count	Squared Euclidean distances are computed after scaling each sample by the total count size factor estimate (Section 2.1).
Sq. Euclidean quantile	Squared Euclidean distances are computed after scaling each sample by the quantile size factor estimate [Section 2.1; Bullard et al. (2010)].
Sq. Euclidean median ratio	Squared Euclidean distances are computed after scaling each sample by the median ratio size factor estimate [Section 2.1; Anders and Huber (2010)].
Poisson total count	The data are transformed as in Section 2.2. Then Poisson dissimilarity is computed according to (17) using the total count size factor estimate (Section 2.1).
Poisson quantile	The data are transformed as in Section 2.2. Then Poisson dissimilarity is computed according to (17) using the quantile size factor estimate [Section 2.1; Bullard et al. (2010)].
Poisson median ratio	The data are transformed as in Section 2.2. Then Poisson dissimilarity is computed according to (17) using the median ratio size factor estimate [Section 2.1; Anders and Huber (2010)].

Finally, Anders and Huber (2010) propose a variance-stabilizing transformation based on the negative binomial model, and suggest performing standard clustering procedures on the transformed data—for instance, one could perform hierarchical clustering after computing the squared Euclidean distances between the transformed observations.

In Sections 5 and 6 we compare our clustering proposal to these competing approaches. Details of the approaches used in the comparisons are given in Table 1.

5. A simulation study.

5.1. *Simulation setup.* We generated data under the model

(18) $X_{ij}|y_i = k \sim \text{NB}(s_i g_j d_{kj}, \phi),$

where ϕ is the dispersion parameter for the negative binomial distribution. Therefore, given that $y_i = k$, X_{ij} has mean $s_i g_j d_{kj}$ and variance $s_i g_j d_{kj} + (s_i g_j d_{kj})^2 \phi$. We tried three values of ϕ: $\phi = 0.01$ (very slight overdispersion), $\phi = 0.1$ (substantial overdispersion), and $\phi = 1$ (very high overdispersion). There were $K = 3$ classes. The size factors are independent and identically distributed, $s_i \sim \text{Unif}(0.2, 2.2)$. The g_j's are independent and identically distributed, $g_j \sim \text{Exp}(1/25)$. Each of the $p = 10{,}000$ features had a 30% chance of being differentially expressed between classes. If a feature was not differentially expressed, then $d_{1j} = d_{2j} = d_{3j} = 1$. If a feature was differentially expressed, then $\log d_{kj} = z_{kj}$ where the z_{kj}'s are independent and identically distributed, $z_{kj} \sim N(0, \sigma^2)$. The value of σ depended on the simulation and is specified in Tables 2 and 3 below.

5.2. *Evaluation of sparse PLDA.* We considered three classifiers:

(1) NSC [Tibshirani et al. (2002, 2003)] after dividing each observation by a size factor estimate.

(2) NSC after dividing each observation by a size factor estimate, and then transforming as follows: $X'_{ij} \leftarrow \sqrt{X_{ij} + 3/8}$. This transformation should make Poisson random variables have approximately constant variance [Anscombe (1948)].

(3) sPLDA after performing the power transformation described in Section 2.2.

For each classifier, three size factor estimates were used: total count, quantile, and median ratio. These are described in Section 2.1. Therefore, a total of nine classification methods were considered. Results are shown in Table 2. sPLDA performs quite well when there is little overdispersion relative to the Poisson model—that is, when the dispersion parameter, ϕ, in the model (18) is small. The performance of sPLDA relative to NSC deteriorates when the data are very overdispersed relative to the Poisson model. Moreover, the square root transformation on the whole seemed to lead to substantially worse results for the NSC classifier.

Interestingly, the choice of size factor estimate (total count, quantile, or median ratio) seems to have little effect on the classifiers' performances, despite the fact that the choice of estimate has been found to play a critical role in the detection of differentially expressed features [Bullard et al. (2010), Robinson and Oshlack (2010), Anders and Huber (2010)]. This is likely because the size factor estimates yield very different results primarily in the setting where a subset of the features containing a large proportion

TABLE 2

Simulation results: nine classification methods. NSC, NSC on $\sqrt{X_{ij} + 3/8}$, and sPLDA were performed, using three different size factor estimates: total count (TC), quantile (Q), and median ratio (MR). Cross-validation was performed on a training set of n observations, and error rates were computed on n test observations. We report the mean numbers of test errors and nonzero features over 50 simulated data sets. Standard errors are in parentheses

n	ϕ	σ	Method	NSC err.	NSC sqrt err.	sPLDA err.	NSC nonzero	NSC sqrt nonzero	sPLDA nonzero
12	0.01	0.05	TC	4.18 (0.34)	5.74 (0.28)	2.24 (0.26)	1947.6 (441.3)	2217.9 (509.0)	791.4 (111.7)
			Q	4.38 (0.34)	5.82 (0.26)	2.26 (0.25)	1670.6 (394.5)	2010.1 (478.2)	782.3 (110.0)
			MR	4.28 (0.34)	5.78 (0.27)	2.20 (0.24)	1731.8 (402.6)	2327.8 (517.9)	795.4 (110.8)
50	0.01	0.025	TC	19.14 (0.67)	24.06 (0.70)	16.84 (0.55)	2316.6 (398.8)	3122.5 (516.6)	1830.7 (217.9)
			Q	20.32 (0.71)	24.82 (0.70)	17.14 (0.56)	1870.7 (335.2)	3380.9 (519.4)	1860.2 (229.6)
			MR	19.66 (0.69)	24.48 (0.69)	16.88 (0.60)	2488.7 (437.8)	2698.7 (513.4)	1934.9 (224.5)
12	0.1	0.1	TC	2.52 (0.31)	2.66 (0.26)	1.58 (0.25)	5143.2 (527.2)	2738.5 (461.2)	3878.2 (369.4)
			Q	2.12 (0.27)	2.68 (0.26)	1.62 (0.26)	5207.0 (536.8)	2879.8 (456.7)	3927.2 (371.7)
			MR	2.28 (0.29)	2.88 (0.28)	1.60 (0.26)	4849.4 (531.2)	2932.0 (477.3)	3889.2 (368.6)
50	0.1	0.05	TC	16.80 (0.54)	17.76 (0.61)	17.94 (0.70)	3802.5 (408.1)	3785.5 (418.1)	3308.5 (355.1)
			Q	17.08 (0.64)	17.16 (0.60)	17.88 (0.65)	4293.2 (479.1)	3921.5 (371.8)	3284.0 (352.8)
			MR	16.78 (0.59)	17.34 (0.66)	17.96 (0.71)	3475.3 (392.4)	4398.3 (457.0)	3489.3 (371.9)
12	1	0.2	TC	3.24 (0.25)	4.28 (0.35)	4.26 (0.32)	8846.2 (380.7)	6127.8 (524.6)	4502.0 (509.9)
			Q	3.20 (0.23)	4.04 (0.33)	4.08 (0.29)	8991.8 (318.8)	6342.1 (557.6)	4551.7 (512.1)
			MR	3.22 (0.26)	3.60 (0.30)	4.00 (0.31)	8389.0 (396.4)	7082.7 (515.5)	4518.9 (514.6)
50	1	0.1	TC	25.56 (0.61)	25.80 (0.55)	25.66 (0.50)	4237.8 (503.5)	4293.5 (495.9)	3150.5 (433.0)
			Q	25.82 (0.61)	25.90 (0.64)	26.02 (0.55)	4629.1 (516.2)	4170.5 (491.7)	3131.2 (406.6)
			MR	25.92 (0.68)	25.86 (0.59)	25.52 (0.51)	4427.5 (524.0)	4362.6 (498.0)	3156.8 (410.4)

TABLE 3

Simulation results: ten clustering methods. Complete-linkage hierarchical clustering was applied to the nine dissimilarity measures described in Table 1, and each dendrogram was cut in order to obtain three clusters. The proposal of Cai et al. (2004) is also included; this required specifying $K = 3$. Mean CERs over 50 simulated data sets are reported, with standard errors in parentheses. The Poisson-based measures perform quite well when overdispersion is low, but tend to be outperformed by EdgeR in the presence of substantial overdispersion

ϕ	σ	Method	Clustering error rate
0.01	0.15	Cai	0.3592 (0.0071)
		Berninger	0.5704 (0.0173)
		EdgeR	0.0000 (0.0000)
		VST	0.6201 (0.0029)
		Squared Euclidean total count	0.5675 (0.0191)
		Squared Euclidean quantile	0.5662 (0.0215)
		Squared Euclidean median ratio	0.5755 (0.0178)
		Poisson total count	0.0045 (0.0045)
		Poisson quantile	0.0057 (0.0047)
		Poisson median ratio	0.0045 (0.0045)
0.1	0.2	Cai	0.3803 (0.0058)
		Berninger	0.1905 (0.0258)
		EdgeR	0.0000 (0.0000)
		VST	0.6204 (0.0029)
		Squared Euclidean total count	0.3051 (0.0327)
		Squared Euclidean quantile	0.2875 (0.0325)
		Squared Euclidean median ratio	0.3297 (0.0350)
		Poisson total count	0.2053 (0.0225)
		Poisson quantile	0.2067 (0.0228)
		Poisson median ratio	0.2006 (0.0219)
1	0.5	Cai	0.3797 (0.0063)
		Berninger	0.5309 (0.0143)
		EdgeR	0.0098 (0.0054)
		VST	0.6058 (0.0089)
		Squared Euclidean total count	0.1630 (0.0242)
		Squared Euclidean quantile	0.2190 (0.0235)
		Squared Euclidean median ratio	0.1998 (0.0305)
		Poisson total count	0.2699 (0.0255)
		Poisson quantile	0.2699 (0.0255)
		Poisson median ratio	0.2749 (0.0254)

of the counts are highly differentially expressed. However, in such a setting, classification tends to be quite easy. In more challenging classification settings in which differentially expressed features have fewer counts and display smaller differences between classes, such as in Table 2, the effect of the size factor estimate appears to play a less important role.

5.3. *Evaluation of Poisson clustering.*   We compare the performances of ten clustering proposals: the K-means clustering proposal of Cai et al. (2004) which assumes a Poisson model, as well as complete-linkage hierarchical clustering applied to the nine dissimilarity measures described in Section 4.2. Cai et al.'s (2004) proposal was performed with $K = 3$ (the true number of clusters), and the hierarchical clustering dendrograms for the other methods were cut at a height that resulted in three clusters.

To evaluate the performances of these clustering methods, we use the clustering error rate (CER), which measures the extent to which two partitions P and Q of a set of n observations disagree. Let $1_{P(i,i')}$ be an indicator for whether observations i and i' are in the same group in partition P, and define $1_{Q(i,i')}$ analogously. Then CER is defined as

$$(19) \qquad \sum_{i > i'} |1_{P(i,i')} - 1_{Q(i,i')}| \Big/ \binom{n}{2}.$$

This is also one minus the Rand Index [Rand (1971)]. We took P to be the true class labels and Q to be the class labels estimated via clustering; a small value indicates an accurate clustering.

Simulation study results with $n = 25$ observations are shown in Table 3. The Poisson clustering proposed in this paper performs well for the full range of overdispersion parameters considered. This is in part because the transformation described in Section 2.2 makes the data approximately Poisson even when the overdispersion parameter ϕ is large. Even though the method of Berninger et al. (2008) is based on a model that is very similar to ours, it exhibits worse performance. This is likely due to numerical issues with their proposal whereby two different observations can have zero dissimilarity and two identical observations can have nonzero dissimilarity. It is difficult to compare the Poisson-based proposal of Cai et al. (2004) directly to the other nine since it uses a K-means approach, where the number of clusters must be specified in advance. Moreover, the proposals of Berninger et al. (2008) and Cai et al. (2004) do not entail first performing a power transformation on the data.

In Table 3 the EdgeR dissimilarity measure exhibited essentially the same performance as our Poisson clustering measure when $\phi = 0.01$, and better performance in the presence of moderate or severe overdispersion. However, it is quite computationally intensive. The example shown in Table 3 contains only 25 observations because running EdgeR using the `Bioconductor` package provided by the authors [Robinson, McCarthy and Smyth (2010)] is too slow for larger values of n. For instance, on a simulated example with $n = 50$ and $p = 10,000$, it took 6 minutes to compute the dissimilarity matrix on a AMD Opteron 848 2.20 GHz processor. In contrast, computing the Poisson dissimilarity matrix on the same example took 14 seconds.

In summary, the Poisson dissimilarity measure outperforms all of the methods besides EdgeR. EdgeR is the overall winner, but is much more computationally demanding.

6. Application to sequencing data sets.

6.1. *Data sets.* We present results based on four data sets. The first three are RNA sequencing data sets, and the fourth is a chromatin immunoprecipitation (ChIP) sequencing data set intended as a preliminary assessment of the extent to which the methods proposed here can be applied to other types of sequencing data.

Liver and kidney. An RNA sequencing data set quantifying the expression of 22,925 genes [Marioni et al. (2008)]. There are seven technical replicates from a liver sample and seven technical replicates from a kidney sample, each from a single human male. The liver and kidney samples are treated as two separate classes. The data are available as a Supplementary File associated with Marioni et al. (2008).

Yeast. An RNA sequencing data set consisting of replicates of *Saccharomyces cerevisiae* (yeast) cultures [Nagalakshmi et al. (2008)]. Three replicates were obtained for each of two library preparation protocols, "random hexamer" (RH) and "oligo(dT)" (dT). For each library preparation protocol, there is an "original" replicate, a "technical" replicate of that original replicate, and also a "biological" replicate. The number of reads mapping to each of 6,874 genes is available as a Supplementary File associated with Anders and Huber (2010). In the analysis that follows, we treat the RH and dT library preparations as two distinct classes.

Cervical cancer. An RNA sequencing data set quantifying the expression of microRNAs in tumor and nontumor human cervical tissue samples [Witten et al. (2010)]. MicroRNAs are small RNAs, 18–30 nucleotides in length, that have been shown to play an important regulatory role in a number of biological processes. The data take the form of 29 tumor and 29 nontumor cervical tissue samples with measurements on 714 microRNAs. Of the tumor samples, 6 are adenocarcinomas (ADC), 21 are squamous cell carcinomas (SCC), and 2 are unclassified. The two unclassified samples are excluded from the analysis. Normal, ADC, and SCC are treated as three separate classes. The data are available from Gene Expression Omnibus [Barrett et al. (2005)] under accession number GSE20592. Since this is a small RNA data set, the experimental protocol differs slightly from the description in Section 1.1: small RNAs were isolated before being converted to cDNA, which was then amplified and sequenced. As pointed out by a reviewer, Linsen et al. (2009) found that small RNA digital gene expression profiling is biased toward certain small RNAs, and so small RNA sequencing data sets cannot be used to accurately determine absolute numbers of small RNAs. However, this bias is systematic and reproducible, and so small RNA se-

quencing data sets can be used to determine relative expression differences between samples. The classification and clustering proposals in this paper rely on relative rather than absolute expression differences in the sense that accurate classification or clustering can be performed even if certain small RNAs contain a disproportionately large number of counts relative to the true abundance in the original sample.

Transcription factor binding. ChIP sequencing is a new approach for mapping protein-DNA interactions at a genome-wide level that relies upon recently developed techniques for high throughput DNA sequencing [Johnson et al. (2007)]. Like RNA sequencing, the results of a ChIP sequencing experiment can be arranged as a $n \times p$ matrix with n observations and p features. The features represent the DNA binding regions for a protein of interest, and the (i, j) element of the data matrix indicates the number of times that the protein was observed to bind to the jth binding region in the ith sample. In Kasowski et al. (2010), the binding sites of RNA polymerase II were mapped in each of ten individuals. 19,061 binding regions were identified, each of which was treated as a distinct feature. At least three replicates were available for each individual, and there were 39 observations in total. This data are available as a Supplementary File associated with Anders and Huber (2010). In what follows, we treat each of the ten individuals as a distinct class.

6.2. *Evaluation of sparse PLDA.* A total of nine classification methods were compared: NSC, NSC on $\sqrt{X_{ij} + 3/8}$, and sPLDA, each with three different size factor estimates. Details are given in Section 5.2. These methods were applied to the four data sets described in Section 6.1. Results on the cervical cancer and transcription factor binding data sets are shown in Figure 2. Results for the liver and kidney data and the yeast data are not shown since on those two data sets, all methods gave 0 cross-validation errors for all of the tuning parameter values considered.

6.3. *Evaluation of Poisson clustering.* We clustered the observations in each of the four data sets described in Section 6.1. Eight dissimilarity measures were used to perform complete-linkage hierarchical clustering (Table 1). The liver and kidney data resulted in a perfect clustering by all methods of comparison (results not shown). The cervical cancer, yeast, and transcription factor binding results are shown in Figures 3, 4 and 5. The cervical cancer data are challenging: the Poisson dissimilarity measures are best able to distinguish between tumor and nontumor samples, but no method is able to convincingly distinguish between ADC and SCC (Figure 3). For the yeast data, all methods but EdgeR and VST yield essentially the same dendrogram—one RH sample appears to be distinct from all the other samples, but the remaining RH and dT samples are quite distinct. For that data, EdgeR and VST yield different (and presumably worse) clusterings.
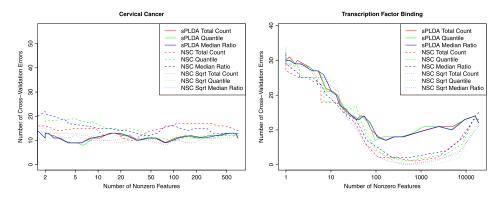
Fɪɢ. 2. *A comparison of classification methods on the cervical cancer data of Witten et al.* *(2010) and the transcription factor binding data of Kasowski et al. (2010). NSC, NSC on the square root transformed data, and sPLDA were performed each with three distinct size factor estimates—total count, quantile [Bullard et al. (2010)], and median ratio [Anders and Huber (2010)], each of which is described in Section 2.1. Five-fold cross-validation was performed. The resulting cross-validation error curves are shown as a function of the number of features included in the classifier. Results for the yeast data of Nagalakshmi et al. (2008) and the liver and kidney data of Marioni et al. (2008) are not shown because all methods gave 0 cross-validation errors for all of the tuning parameter values considered.*
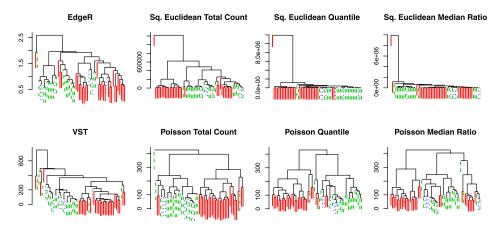

Fɪɢ. 3. *Complete-linkage hierarchical clustering dendrograms obtained by computing eight dissimilarity measures on the cervical cancer data of Witten et al. (2010). The dissimilarity measures are described in Table 1. Normal samples are shown as red solid lines, ADC as blue dotted lines, and SCC as green dashed lines. The Poisson-based approaches seem to do the best job of separating the normal samples from the tumor samples.*

The transcription factor binding data are the most complex since there are ten groups (one per individual). There is no clear winner, but EdgeR seems to perform quite well (Figure 5). The CERs for each dendrogram can be found in Figure 6.
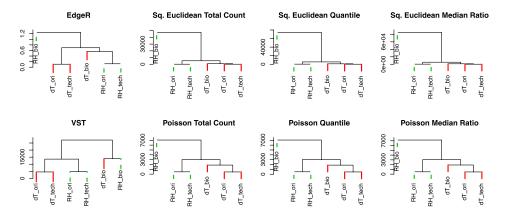
Fig. 4. *Complete-linkage hierarchical clustering dendrograms obtained by computing eight dissimilarity measures on the yeast data of Nagalakshmi et al. (2008). The dissimilarity measures are described in Table 1. The dT samples are shown in red and RH samples are in green. The three methods based on Euclidean distance and the three methods based on Poisson dissimilarity give the most accurate dendrograms on this data, since they successfully group the dT samples together.*
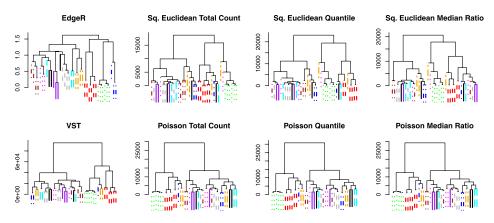

Fig. 5. *Complete-linkage hierarchical clustering dendrograms obtained by computing eight dissimilarity measures on the transcription factor binding data of Kasowski et al. (2010). The dissimilarity measures are described in Table 1. Replicates from each of the ten individuals are shown in a different color.*

7. Discussion. In this paper we have proposed approaches for the classification and clustering of sequencing data. As sequencing technologies become increasingly widespread, the importance of statistical methods that are well suited to this type of data will increase. The approaches proposed in this paper were designed for RNA sequencing data, but could likely be extended to other sequencing technologies such as DNA and ChIP sequencing. In fact, an application to ChIP sequencing data was presented in Section 6.
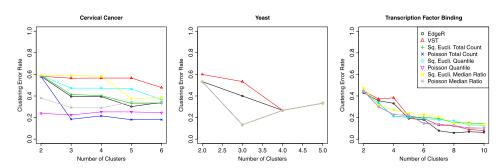
FIG. 6. *For each of the eight dissimilarity measures described in Table 1, the figure displays the CERs that result from cutting the complete linkage hierarchical clustering dendrogram at various cutpoints.*

The methods proposed in this paper follow naturally from a simple Poisson log linear model (3) for sequencing data. Similar approaches could be taken using an alternative model, for instance, one based on the negative binomial distribution. The methods proposed seem to work very well if the true model for the data is Poisson or if there is mild overdispersion relative to the Poisson model. Performance degrades in the presence of severe overdispersion. Most sequencing data seem to be somewhat overdispersed relative to the Poisson model. It may be that extending the approaches proposed here to the negative binomial model could result in improved performance in the presence of overdispersion.

A number of authors have proposed detecting differentially expressed features in sequencing data by making inference on a Poisson log linear model [see, e.g., Marioni et al. (2008), Bullard et al. (2010), Li et al. (2011)]. In this paper we have used such a model to develop proposals for classification and clustering. However, many other types of inference based on sequencing data are likely to be of interest in the future. For instance, in a recent paper, Lee, Huang and Hu (2010) proposed a method for performing principal components analysis (PCA) for high-dimensional binary data. In a similar vein, one could develop an approach for PCA for sequencing data using the Poisson log linear model (1). We leave this as a topic for further research.

It has been shown that the manner in which samples are normalized is of great importance in identifying differentially expressed features on the basis of sequencing data [Bullard et al. (2010), Robinson and Oshlack (2010), Anders and Huber (2010)]. However, in Sections 5 and 6, the normalization approach appeared to have little effect on the results obtained. This seems to be due to the fact that the choice of normalization approach is most important when a few features with very high counts are differentially expressed between classes. In that case, identification of differentially expressed features can be challenging, but classification and clustering are quite straightforward.

It is known that RNA-sequencing data suffer from *transcript length bias*—that is, longer transcripts tend to result in a greater number of reads, resulting in an increased tendency to call such transcripts differentially expressed [Oshlack and Wakefield (2009)]. In a similar manner, the classification and clustering proposals made in this paper are affected by the total number of counts per feature; this can be seen by inspection of (7), (11) and (17). It seems clear that bias due to the total number of counts per feature is undesirable for the task of identifying differentially expressed transcripts, since it makes it difficult to detect differential expression for low-frequency transcripts. However, it is not clear that such a bias is undesirable in the case of classification or clustering, since we would like features about which we have the most information—namely, the features with the highest total counts—to have the greatest effect on the classifiers and dissimilarity measures that we use. More investigation into this matter is left as a topic for future work.

Our proposal for clustering sequencing data is based on the development of a dissimilarity measure that is potentially more appropriate for count data than standard Euclidean distance. The resulting dissimilarity matrix can then be input to a standard clustering algorithm, such as hierarchical clustering. Other statistical techniques that rely upon a dissimilarity matrix, such as multidimensional scaling, could also be performed using the Poisson dissimilarity measure developed here.

An R language package implementing the methods proposed in this paper will be made available.

APPENDIX A: PROPERTIES OF THE POISSON DISSIMILARITY MEASURE

We wish to prove that the dissimilarity between $\mathbf{x}_i$ and $\mathbf{x}_{i'}$ specified in (17) is nonnegative, and that it equals zero when $\mathbf{x}_i = \mathbf{x}_{i'}$.

To prove nonnegativity, first notice that $g(d_{ij}) = -\hat{N}_{ij}d_{ij} + X_{ij}\log d_{ij}$ is a concave function of d_{ij}, and is maximized when $d_{ij} = \frac{X_{ij}}{\hat{N}_{ij}}$. Therefore, $g(\frac{X_{ij}}{\hat{N}_{ij}}) \geq g(1)$. And since $\frac{X_{ij}+\beta}{\hat{N}_{ij}+\beta}$ is between 1 and $\frac{X_{ij}}{\hat{N}_{ij}}$, concavity of g ensures that $g(\frac{X_{ij}+\beta}{\hat{N}_{ij}+\beta}) \geq g(1)$; that is, $\hat{N}_{ij} - \hat{N}_{ij}d_{ij} + X_{ij}\log d_{ij} \geq 0$. It follows directly that (17) is nonnegative.

Now, if $\mathbf{x}_i = \mathbf{x}_{i'}$, then $\hat{N}_{ij} = \hat{N}_{i'j} = X_{ij} = X_{i'j}$ and so by (16), $\hat{d}_{ij} = \hat{d}_{i'j} = 1$. By inspection, (17) equals zero.

APPENDIX B: EQUIVALENCE OF LOG LIKELIHOOD RATIO STATISTICS UNDER POISSON MODEL AND MULTINOMIAL MODEL

Here, we show that the log likelihood ratio statistic (17) under the Poisson model is identical to the log likelihood ratio statistic under the model of

Berninger et al. ([2008](#)), if appropriate estimates of N_{ij}, $N_{i'j}$, d_{ij}, and $d_{i'j}$ are used in (17).

In Section 4.1 we assumed that the ith and i'th observations take the form $X_{ij} \sim \text{Poisson}(N_{ij}d_{ij})$, $X_{i'j} \sim \text{Poisson}(N_{i'j}d_{i'j})$, $N_{ij} = s_i g_j$, $N_{i'j} = s_{i'} g_j$. Under the null hypothesis, $d_{ij} = d_{i'j} = 1$. Under the alternative, d_{ij} and $d_{i'j}$ are unconstrained. Suppose we estimate N_{ij} and $N_{i'j}$ under the null using the MLEs, or, equivalently, using the total count size factor estimates given in Section 2.1: then $\hat{N}_{ij} = X_{i\cdot}(X_{ij} + X_{i'j})/(X_{i\cdot} + X_{i'\cdot})$, $\hat{N}_{i'j} = X_{i'\cdot}(X_{ij} + X_{i'j})/(X_{i\cdot} + X_{i'\cdot})$. Treating these estimates as offsets under the alternative, the MLE for d_{ij} is X_{ij}/N_{ij}, and the MLE for $d_{i'j}$ is $X_{ij}/N_{i'j}$. Plugging these estimates into (17) yields

$$\sum_{j=1}^{p} (X_{i\cdot}(X_{ij} + X_{i'j})/(X_{i\cdot} + X_{i'\cdot}) + X_{i'\cdot}(X_{ij} + X_{i'j})/(X_{i\cdot} + X_{i'\cdot})$$

$$- X_{ij} - X_{i'j} + X_{ij}\log(X_{ij}/N_{ij}) + X_{i'j}\log(X_{i'j}/N_{i'j}))$$

$$(20) \qquad = \sum_{j=1}^{p} (X_{ij}\log(X_{ij}/N_{ij}) + X_{i'j}\log(X_{i'j}/N_{i'j}))$$

$$= \sum_{j=1}^{p} (X_{ij}\log X_{ij} + X_{i'j}\log X_{i'j} - (X_{ij} + X_{i'j})\log(X_{ij} + X_{i'j}))$$

$$+ (X_{i\cdot} + X_{i'\cdot})\log(X_{i\cdot} + X_{i'\cdot}) - X_{i\cdot}\log X_{i\cdot} - X_{i'\cdot}\log X_{i'\cdot}.$$

Now, Berninger et al. ([2008](#)) instead assume a multinomial model for the data: $X_{i1}, \ldots, X_{ip} \sim \text{Multinomial}(X_{i\cdot}, q_1, \ldots, q_p)$ and $X_{i'1}, \ldots, X_{i'p} \sim \text{Multinomial}(X_{i'\cdot}, r_1, \ldots, r_p)$. Under the null, $q_j = r_j \ \forall j$. Under the alternative, q_j and r_j are unconstrained. This results in the likelihood ratio statistic

$$(21) \qquad \prod_{j=1}^{p} \frac{(X_{ij}/X_{i\cdot})^{X_{ij}}(X_{i'j}/X_{i'\cdot})^{X_{i'j}}}{((X_{ij} + X_{i'j})/(X_{i\cdot} + X_{i'\cdot}))^{X_{ij}+X_{i'j}}}.$$

Taking the logarithm of (21) yields (20).

Note that, in practice, the dissimilarity measures proposed in Section 4.1 and in Berninger et al. ([2008](#)) are not identical, since in Section 4.1 we estimate d_{ij} and $d_{i'j}$ as the posterior means using a Gamma prior. Berninger et al. ([2008](#)) instead use a Dirichlet prior on $q_1, \ldots, q_p$ and $r_1, \ldots, r_p$ and use the Bayes factor as the dissimilarity measure. In fact, the proposal of Berninger et al. ([2008](#)) seems to perform substantially worse than that of Section 4.1 in the simulation study in Section 5.

(2008), to Li Cai for providing command line software for the proposal described in Cai et al. (2004), and to Mark Robinson for helpful responses to inquiries regarding the Bioconductor package edgeR [Robinson, McCarthy and Smyth (2010)]. An Associate Editor and two referees provided comments that greatly improved the quality of this paper.

REFERENCES

Agresti, A. (2002). *Categorical Data Analysis*. Wiley, Hoboken, NJ.

Anders, S. and Huber, W. (2010). Differential expression analysis for sequence count data. *Genome Biol.* **11** R106.

Anscombe, F. J. (1948). The transformation of Poisson, binomial and negative-binomial data. *Biometrika* **35** 246–254. MR0028556

Auer, P. L. and Doerge, R. W. (2010). Statistical design and analysis of RNA sequencing data. *Genetics* **185** 405–416.

Barrett, T., Suzek, T. O., Troup, D. B., Wilhite, S. E., Ngau, W.-C., Ledoux, P., Rudnev, D., Lash, A. E., Fujibuchi, W. and Edgar, R. (2005). NCBI GEO: Mining millions of expression profiles–database and tools. *Nucleic Acids Res.* **33** D562–D566.

Berninger, P., Gaidatzis, D., van Nimwegen, E. and Zavolan, M. (2008). Computational analysis of small RNA cloning data. *Methods* **44** 13–21.

Bickel, P. J. and Levina, E. (2004). Some theory of Fisher's linear discriminant function, 'naive Bayes', and some alternatives when there are many more variables than observations. *Bernoulli* **10** 989–1010. MR2108040

Brown, P. and Botstein, D. (1999). Exploring the new world of the genome with DNA microarrays. *Nature Genetics* **21** 33–37.

Bullard, J. H., Purdom, E., Hansen, K. D. and Dudoit, S. (2010). Evaluation of statistical methods for normalization and differential expression in mRNA-Seq experiments. *BMC Bioinformatics* **11** 94.

Cai, L., Huang, H., Blackshaw, S., Liu, J., Cepko, C. and Wong, W. (2004). Clustering analysis of SAGE data using a Poisson approach. *Genome Biology* **5** R51.

DeRisi, J., Iyer, V. and Brown, P. (1997). Exploring the metabolic and genetic control of gene expression on a genomic scale. *Science* **278** 680–686.

Dudoit, S., Fridlyand, J. and Speed, T. P. (2001). Comparison of discrimination methods for the classification of tumors using gene expression data. *J. Amer. Statist. Assoc.* **96** 1151–1160.

Hastie, T., Tibshirani, R. and Friedman, J. (2009). *The Elements of Statistical Learning: Data Mining, Inference, and Prediction*. Springer, New York.

Johnson, D. S., Mortazavi, A., Myers, R. M. and Wold, B. (2007). Genome-wide mapping of in vivo protein-DNA interactions. *Science* **316** 1497–1502.

Kasowski, M., Grubert, F., Heffelfinger, C., Hariharan, M., Asabere, A., Waszak, S. M., Habegger, L., Rozowsky, J., Shi, M., Urban, A. E., Hong, M.-Y., Karczewski, K. J., Huber, W., Weissman, S. M., Gerstein, M. B., Korbel, J. O. and Snyder, M. (2010). Variation in transcription factor binding among humans. *Science* **328** 232–235.

Lee, S., Huang, J. Z. and Hu, J. (2010). Sparse logistic principal components analysis for binary data. *Ann. Appl. Stat.* **4** 1579–1601.

Li, J., Witten, D., Johnstone, I. and Tibshirani, R. (2011). Normalization, testing, and false discovery rate estimation for RNA-sequencing data. *Biostatistics*. To appear.

Linsen, S. E. V., de Wit, E., Janssens, G., Heater, S., Chapman, L., Parkin, R. K., Fritz, B., Wyman, S. K., de Bruijn, E., Voest, E. E., Kuersten, S., Tewari, M.

and Cuppen, E. (2009). Limitations and possibilities of small RNA digital gene expression profiling. *Nature Methods* **6** 474–476.

Marioni, J. C., Mason, C. E., Mane, S. M., Stephens, M. and Gilad, Y. (2008). RNA-seq: An assessment of technical reproducibility and comparison with gene expression arrays. *Genome Res.* **18** 1509–1517.

Monti, S., Savage, K. J., Kutok, J. L., Feuerhake, F., Kurtin, P., Mihm, M., Wu, B., Pasqualucci, L., Neuberg, D., Aguiar, R. C. T., Cin, P. D., Ladd, C., Pinkus, G. S., Salles, G., Harris, N. L., Dalla-Favera, R., Habermann, T. M., Aster, J. C., Golub, T. R. and Shipp, M. A. (2005). Molecular profiling of diffuse large B-cell lymphoma identifies robust subtypes including one characterized by host inflammatory response. *Blood* **105** 1851–1861.

Morozova, O., Hirst, M. and Marra, M. A. (2009). Applications of new sequencing technologies for transcriptome analysis. *Annu. Rev. Genomics Hum. Genet.* **10** 135–151.

Mortazavi, A., Williams, B. A., McCue, K., Schaeffer, L. and Wold, B. (2008). Mapping and quantifying mammalian transcriptomes by RNA-Seq. *Nature Methods* **5** 621–628.

Nagalakshmi, U., Wong, Z., Waern, K., Shou, C., Raha, D., Gerstein, M. and Snyder, M. (2008). The transcriptional landscape of the yeast genome defined by RNA sequencing. *Science* **302** 1344–1349.

Nielsen, T., West, R., Linn, S., Alter, O., Knowling, M., O'Connell, J. S. Z., Fero, M., Sherlock, G., Pollack, J., Brown, P., Botstein, D. and van de Rijn, M. (2002). Molecular characterisation of soft tissue tumours: A gene expression study. *The Lancet* **359** 1301–1307.

Oshlack, A., Robinson, M. and Young, M. (2010). From RNA-seq reads to differential expression results. *Genome Biology* **11** 220.

Oshlack, A. and Wakefield, M. (2009). Transcript length bias in RNA-seq data confounds system biology. *Biology Direct* **4** 14.

Pepke, S., Wold, B. and Mortazavi, A. (2009). Computation for ChIP-seq and RNA-seq studies. *Nature Methods* **6** S22–S32.

Ramaswamy, S., Tamayo, P., Rifkin, R., Mukherjee, S., Yeang, C., Angelo, M., Ladd, C., Reich, M., Latulippe, E., Mesirov, J., Poggio, T., Gerald, W., Loda, M., Lander, E. and Golub, T. (2001). Multiclass cancer diagnosis using tumor gene expression signature. *PNAS* **98** 15149–15154.

Rand, W. M. (1971). Objective criteria for the evaluation of clustering methods. *J. Amer. Statist. Assoc.* **66** 846–850.

Robinson, M. D., McCarthy, D. J. and Smyth, G. K. (2010). edgeR: A Bioconductor package for differential expression analysis of digital gene expression data. *Bioinformatics* **26** 139–140.

Robinson, M. D. and Oshlack, A. (2010). A scaling normalization method for differential expression analysis of RNA-seq data. *Genome Biol.* **11** R25.

Spellman, P. T., Sherlock, G., Iyer, V. R., Zhang, M., Anders, K., Eisen, M. B., Brown, P. O., Botstein, D. and Futcher, B. (1998). Comprehensive identification of cell cycle-reulated genes of the yeast saccharomyces by microarray hybridization. *Mol. Cell. Biol.* **9** 3273–3975.

Tibshirani, R., Hastie, T., Narasimhan, B. and Chu, G. (2002). Diagnosis of multiple cancer types by shrunken centroids of gene expression. *Proc. Natl. Acad. Sci. USA* **99** 6567–6572.

TIBSHIRANI, R., HASTIE, T., NARASIMHAN, B. and CHU, G. (2003). Class prediction by nearest shrunken centroids, with applications to DNA microarrays. *Statist. Sci.* **18** 104–117. MR1997067

WANG, S. M. (2007). Understanding SAGE data. *Trends Genet.* **23** 42–50.

WANG, Z., GERSTEIN, M. and SNYDER, M. (2009). RNA-Seq: A revolutionary tool for transcriptomics. *Nat. Rev. Genet.* **10** 57–63.

WILHELM, B. T. and LANDRY, J.-R. (2009). RNA-Seq-quantitative measurement of expression through massively parallel RNA-sequencing. *Methods* **48** 249–257.

WITTEN, D. and TIBSHIRANI, R. (2011). Penalized classification using Fisher's linear discriminant. *J. Roy. Statist. Soc. Ser. B* **73** 753–772.

WITTEN, D., TIBSHIRANI, R., GU, S., FIRE, A. and LUI, W. (2010). Ultra-high throughput sequencing-based small RNA discovery and discrete statistical biomarker analysis in a collection of cervical tumous and matched controls. *BMC Biology* **8** 58.

DEPARTMENT OF BIOSTATISTICS
UNIVERSITY OF WASHINGTON
BOX 357232
SEATTLE, WASHINGTON 98195-7232
USA
E-MAIL: dwitten@u.washington.edu